

# SCET sum rules for heavy-to-light form factors

Junegone Chay,<sup>1,\*</sup> Chul Kim,<sup>2,†</sup> and Adam K. Leibovich<sup>2,‡</sup>

<sup>1</sup>*Department of Physics, Korea University, Seoul 136-701, Korea*

<sup>2</sup>*Department of Physics and Astronomy,  
University of Pittsburgh, PA 15260, U.S.A.*

(Dated: August 27, 2018)

## Abstract

We consider a sum rule for heavy-to-light form factors in soft-collinear effective theory (SCET). Using the correlation function given by the time-ordered product of a heavy-to-light current and its hermitian conjugate, the heavy-to-light soft form factor  $\zeta_P$  can be related to the leading-order  $B$  meson shape function. Using the scaling behavior of the heavy-to-light form factor in  $\Lambda_{\text{QCD}}/m_b$ , we put a constraint on the behavior of the  $B$  meson shape function near the endpoint. We employ the sum rule to estimate the size of  $\zeta_P$  with the model for the shape function and find that it ranges from 0.01 to 0.07.

PACS numbers: 11.55.Hx, 13.25.Hw

Keywords: soft-collinear effective theory, sum rule, heavy-to-light form factor

---

\*Electronic address: chay@korea.ac.kr

†Electronic address: chk30@pitt.edu

‡Electronic address: akl2@pitt.edu

Information on heavy-to-light form factors is important to extract Standard Model parameters from experimental results. For instance, the  $B \rightarrow \pi$  form factor is needed to extract  $V_{ub}$  or the CKM angle  $\gamma$  from exclusive  $B$  decays [1]. Due to the non-perturbative nature of the form factor, techniques beyond perturbation theory need to be employed to try to evaluate these functions. Unquenched lattice results are starting to be available for the  $B \rightarrow \pi$  form factor [2]. Due to the uncertainties in the lattice technique, the pion is restricted to have energies  $E_\pi \lesssim 1$  GeV, just in the region where the experimental uncertainty is largest. Another method for determining the form factor is light-cone sum rules [3]. In Ref. [4] (see also [5]), light-cone sum rules were investigated using soft-collinear effective theory (SCET) [6], where it is argued that using SCET allows for a more consistent scheme to calculate both factorizable and non-factorizable contributions than the traditional light-cone sum rule approach.

In this paper, we investigate a novel sum rule using SCET, relating the  $B \rightarrow \pi$  form factor at small  $q^2$  to the  $B$  meson shape function [7] which describes the motion of the  $b$  quark inside the  $B$  meson. The shape function cannot be calculated, but it can be extracted from the data [8]. After relating the two non-perturbative functions using the sum rule, we use the scaling in  $\Lambda_{\text{QCD}}/m_b$  of the  $B \rightarrow \pi$  form factor to put constraints on shape function models near the endpoint region. By choosing a model for a shape function which satisfies the constraints, we can give model-dependent values for the  $B \rightarrow \pi$  form factor at  $q^2 = 0$ .

Let us consider the correlation function in SCET<sub>I</sub> [9], defined as

$$\Pi(q) = i \int d^4z e^{iq \cdot z} \langle \bar{B} | T[J_0^\dagger(z) J_0(0)] | \bar{B} \rangle, \quad (1)$$

where the leading-order heavy-to-light current in SCET can be written as

$$J_0(x) = e^{i(\tilde{p} - m_b v) \cdot x} \bar{\xi}_n W Y^\dagger h_v(x). \quad (2)$$

Here  $\tilde{p} = \bar{n} \cdot p n^\mu / 2 + p_\perp^\mu$  is the label momentum of the collinear quark  $\xi_n$ , which has momentum  $p^\mu = \tilde{p}^\mu + k^\mu$ , and we will set  $p_\perp^\mu = 0$ . We are interested in the correlation function under the same kinematic condition as the forward scattering amplitude of inclusive  $B$  decays in the endpoint region. We denote the residual momentum  $r$  as the remainder of the sum of large momenta of the heavy quark, the collinear quark, and the incoming momentum  $q$ , with

$$r^\mu = m_b v + q^\mu - \tilde{p}^\mu \sim \mathcal{O}(\Lambda), \quad n \cdot r = n \cdot q + m_b, \quad \bar{n} \cdot r = r_\perp = 0. \quad (3)$$

$n \cdot q$  is chosen to be negative, and  $\Lambda$  is a typical hadronic scale. Since  $n \cdot r$  is of order  $\Lambda$ , the quark field in the intermediate state becomes hard-collinear with  $p^2 \sim \mathcal{O}(m_b \Lambda)$ . If we take a cut of the correlation function  $\Pi(q)$ , the final state contains a pion or other collinear particles which include a hard-collinear quark and an ultrasoft (usoft) quark. The Feynman diagram for the correlation function at leading order is schematically shown in Fig. 1.

The dispersion relation of the correlation function can be written as

$$\Pi[(p_B + q')^2] = \frac{1}{\pi} \int_{m_\pi^2}^{\infty} d(p_B + q)^2 \frac{\text{Im}\Pi[(p_B + q)^2]}{(p_B + q)^2 - (p_B + q')^2 - i\epsilon}, \quad (4)$$

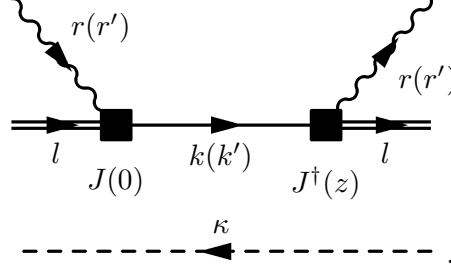


FIG. 1: Feynman diagram for the correlation function  $\Pi$  in the timelike (spacelike) region. The double line is a heavy quark field, the solid line is a hard-collinear quark with the residual momentum  $k(k')$ . The dashed line is a spectator quark in the  $B$  meson, which is a soft field in SCET<sub>I</sub>.

where  $p_B$  is the momentum of the  $B$  meson. With  $\bar{\Lambda} = m_B - m_b$ , we can write

$$\begin{aligned} (p_B + q)^2 &= (m_B v + q)^2 = [(m_b + \bar{\Lambda})v + q]^2 \\ &= \bar{n} \cdot p(n \cdot r + \bar{\Lambda}) + \mathcal{O}(\Lambda^2), \end{aligned} \quad (5)$$

and similarly  $(p_B + q')^2 = \bar{n} \cdot p(n \cdot r' + \bar{\Lambda}) + \mathcal{O}(\Lambda^2)$ . The pion mass is regarded as  $m_\pi^2 \sim \Lambda^2$ . In terms of the residual momentum  $n \cdot r$ , the dispersion relation is

$$\Pi(n \cdot r') = \frac{1}{\pi} \int_{m_\pi^2/\bar{n} \cdot p - \bar{\Lambda}}^{\infty} dn \cdot r \frac{\text{Im}\Pi(n \cdot r)}{n \cdot r - n \cdot r' - i\epsilon}. \quad (6)$$

In the lower bound of the integral,  $m_\pi^2/\bar{n} \cdot p$  can be neglected compared to  $\bar{\Lambda}$ .

Using the optical theorem, the correlation function in the timelike region can be written as

$$2 \text{Im}\Pi(r) = \sum_X \int \mathcal{D} \prod_X e^{iq \cdot z} \langle \bar{B} | J_0^\dagger(z) | X \rangle \langle X | J_0(0) | \bar{B} \rangle = 2 \text{Im}\Pi^S + 2 \text{Im}\Pi^C, \quad (7)$$

where the superscripts ‘S’ and ‘C’ mean the contributions from the single-pion state and from the continuum state respectively. The imaginary part of the correlation function from the single-pion state is given by

$$2 \text{Im}\Pi^S = \int \frac{d^3 p_\pi}{(2\pi)^3} \frac{1}{2E_\pi} (2\pi)^4 \delta(p_B + q - p_\pi) \langle \bar{B} | J_0^\dagger | \pi_n \rangle \langle \pi_n | J_0 | \bar{B} \rangle, \quad (8)$$

where the matrix element between the  $B$  meson and the energetic pion  $\pi_n$  is expressed in term of the heavy-to-light form factor

$$\langle \pi_n | J_0 | \bar{B} \rangle = \bar{n} \cdot p \zeta_P(\mu). \quad (9)$$

Therefore the correlation function for the single pion in the timelike region can be written as

$$2 \text{Im}\Pi^S = 2\pi \delta((p_B + q)^2 - m_\pi^2) (\bar{n} \cdot p)^2 \zeta_P^2(\mu) \sim 2\pi \delta((p_B + q)^2) (\bar{n} \cdot p)^2 \zeta_P^2(\mu). \quad (10)$$

Using Eqs. (4), (5), and (10), the dispersion relation Eq. (6) can be rewritten as

$$\Pi(n \cdot r') = \frac{\bar{n} \cdot p \zeta_P^2}{-\bar{\Lambda} - n \cdot r' - i\epsilon} + \frac{1}{\pi} \int_{w'_s}^{\infty} dw \frac{\text{Im}\Pi(w)}{w - n \cdot r' - i\epsilon}, \quad (11)$$

where  $w = n \cdot r$  and  $w'_s = 4m_\pi^2/\bar{n} \cdot p - \bar{\Lambda}$  is related to the onset of the continuum states, which we take as  $s_0 = 4m_\pi^2 = \bar{n} \cdot p(w'_s + \bar{\Lambda})$ .

At the parton level, the correlation function  $\Pi(n \cdot r')$  can be obtained from SCET. From the matching between SCET<sub>I</sub> and SCET<sub>II</sub>, the time-ordered product of the heavy-to-light current and its hermitian conjugate can be expressed in terms of the jet function and the  $B$  meson shape function in SCET<sub>II</sub>. Starting from Eq. (1), the correlation function is

$$\begin{aligned} \Pi(n \cdot r') &= -m_B \int \frac{d\bar{n} \cdot z}{4\pi} \int dn \cdot k e^{i(n \cdot r' - n \cdot k)\bar{n} \cdot z/2} J_P(n \cdot k) \\ &\quad \times \langle \bar{B}_v | \bar{h} Y \left( \frac{\bar{n} \cdot z}{2} \right) \frac{\not{n}}{2} Y^\dagger h(0) | \bar{B}_v \rangle, \end{aligned} \quad (12)$$

where the jet function  $J_P$  with  $P = \bar{n} \cdot p$  is defined as

$$\langle 0 | T W^\dagger \xi_n(z) \bar{\xi} W(0) | 0 \rangle = i \frac{\not{n}}{2} \delta(n \cdot z) \delta(z_\perp) \int \frac{dn \cdot k}{2\pi} e^{-in \cdot k' \bar{n} \cdot z/2} J_P(n \cdot k). \quad (13)$$

The jet function can be computed perturbatively and at tree level it is given by

$$J_P^{(0)}(n \cdot k) = \frac{1}{n \cdot k + i\epsilon}. \quad (14)$$

The  $B$  meson shape function is defined as

$$\begin{aligned} \langle \bar{B}_v | \bar{h} Y \left( \frac{\bar{n} \cdot z}{2} \right) Y^\dagger h(0) | \bar{B}_v \rangle &= \int dn \cdot l e^{in \cdot l \bar{n} \cdot z/2} \langle \bar{B}_v | \bar{h} Y \delta(n \cdot l - n \cdot i\partial) Y^\dagger h | \bar{B}_v \rangle \\ &= \int dn \cdot l e^{in \cdot l \bar{n} \cdot z/2} f(n \cdot l) \text{Tr} \frac{1 + \not{\bar{n}}}{2} \\ &= 2 \int dn \cdot l e^{in \cdot l \bar{n} \cdot z/2} f(n \cdot l), \end{aligned} \quad (15)$$

where the residual momentum  $n \cdot l$  should be less than  $\bar{\Lambda}$  since the shape function has support for  $n \cdot l \leq \bar{\Lambda}$ . Because  $n \cdot k = n \cdot l + n \cdot r'$  from the phase space integral in Eq. (12), the correlation function can be written as

$$\Pi(n \cdot r') = -m_B \int_{-\infty}^{\bar{\Lambda}} dn \cdot l f(n \cdot l) J_P(n \cdot l + n \cdot r' + i\epsilon). \quad (16)$$

At tree level, the correlation function becomes

$$\Pi(n \cdot r') = m_B \int_{-\bar{\Lambda}}^{\infty} dw \frac{f(-w = n \cdot l)}{w - n \cdot r' - i\epsilon}, \quad (17)$$

where we have changed the integral variable to  $w = -n \cdot l$  to allow for an easier comparison with Eq. (11).

From Eqs. (11) and (17), we obtain the tree-level relation

$$m_B \int_{-\bar{\Lambda}}^{\infty} dw \frac{f(-w)}{w - n \cdot r' - i\epsilon} = \frac{\bar{n} \cdot p \zeta_P^2}{-\bar{\Lambda} - n \cdot r' - i\epsilon} + \frac{1}{\pi} \int_{w'_s}^{\infty} dw \frac{\text{Im}\Pi(w)}{w - n \cdot r' - i\epsilon}. \quad (18)$$

Taking a Borel transformation on each side of Eq. (18), we obtain

$$m_B \int_{-\bar{\Lambda}}^{\infty} dw f(-w) e^{-w/w_M} = \bar{n} \cdot p \zeta_P^2 e^{\bar{\Lambda}/w_M} + \frac{1}{\pi} \int_{w'_s}^{\infty} dw \text{Im}\Pi(w) e^{-w/w_M}. \quad (19)$$

From this relation, we can relate the heavy-to-light form factor to the  $B$  meson shape function as

$$\begin{aligned} \zeta_P^2 &= \frac{1}{\bar{n} \cdot p} \left[ m_B \int_{-\bar{\Lambda}}^{\infty} dw f(-w) e^{-(w+\bar{\Lambda})/w_M} - \frac{1}{\pi} \int_{w'_s}^{\infty} dw \text{Im}\Pi(w) e^{-(w+\bar{\Lambda})/w_M} \right] \\ &= \frac{m_B}{\bar{n} \cdot p} \left[ \int_{-\bar{\Lambda}}^{\infty} dw f(-w) e^{-(w+\bar{\Lambda})/w_M} - \int_{w'_s}^{\infty} dw f(-w) e^{-(w+\bar{\Lambda})/w_M} \right] \\ &= \frac{m_B}{\bar{n} \cdot p} \int_{-\bar{\Lambda}}^{w'_s} dw f(-w) e^{-(w+\bar{\Lambda})/w_M}. \end{aligned} \quad (20)$$

By changing the variable  $w + \bar{\Lambda} \rightarrow w$ , we finally obtain our main result

$$\zeta_P^2 = \frac{m_B}{\bar{n} \cdot p} \int_0^{w_s} dw f(\bar{\Lambda} - w) e^{-w/w_M}, \quad (21)$$

where the Borel parameter  $w_M$  is given by  $M^2 = w_M \bar{n} \cdot p \sim m_b \Lambda$  with  $w_M \sim \Lambda_{\text{QCD}}$ . The other parameter  $w_s$  is given by  $w_s = w'_s + \bar{\Lambda}$  with  $s_0 = 4m_\pi^2 = w_s \bar{n} \cdot p$ . Note that  $w_s$  is a measure of the distance to the continuum and is roughly of order  $\Lambda_{\text{QCD}}^2/m_b$ .

When we expand the integrand in a Taylor series near  $w = 0$ , Eq. (21) becomes

$$\begin{aligned} \zeta_P^2 &= \frac{m_B}{\bar{n} \cdot p} \int_0^{w_s} dw \left\{ f(\bar{\Lambda}) - w \left[ f'(\bar{\Lambda}) + \frac{f(\bar{\Lambda})}{w_M} \right] + \frac{w^2}{2} \left[ f''(\bar{\Lambda}) + \frac{2f'(\bar{\Lambda})}{w_M} + \frac{f(\bar{\Lambda})}{w_M^2} \right] + \dots \right\} \\ &= \frac{m_B}{\bar{n} \cdot p} \left\{ f(\bar{\Lambda}) w_s - \frac{w_s^2}{2} \left[ f'(\bar{\Lambda}) + \frac{f(\bar{\Lambda})}{w_M} \right] + \frac{w_s^3}{6} \left[ f''(\bar{\Lambda}) + \frac{2f'(\bar{\Lambda})}{w_M} + \frac{f(\bar{\Lambda})}{w_M^2} \right] + \dots \right\}. \end{aligned} \quad (22)$$

Since  $f(\bar{\Lambda}) = 0$ , Eq. (22) simplifies to

$$\zeta_P^2 = \frac{m_B}{\bar{n} \cdot p} \left\{ -\frac{w_s^2}{2} f'(\bar{\Lambda}) + \frac{w_s^3}{6} \left[ f''(\bar{\Lambda}) + \frac{2f'(\bar{\Lambda})}{w_M} \right] + \dots \right\}. \quad (23)$$

From various arguments [10, 11] the soft form factor  $\zeta_P$  scales as  $(\Lambda_{\text{QCD}}/m_b)^{3/2}$ , which puts a constraint on the behavior of the  $B$  meson shape function near  $\bar{\Lambda}$ , though the functional form is unknown. Since the left-hand side scales as  $(\Lambda_{\text{QCD}}/m_b)^3$ , we can constrain the scaling of the terms on the right-hand side. With  $w_s \sim \Lambda^2/m_b$ , the shape function  $f(\bar{\Lambda})$  and its derivatives of  $f(\bar{\Lambda})$  should scale as  $f(\bar{\Lambda}) \sim \Lambda$ ,  $f'(\bar{\Lambda}) \sim 1/\Lambda$ ,  $f''(\bar{\Lambda}) \sim 1/\Lambda^3$ ,  $\dots$ , based on Eq. (22). In general the shape function has a width of order  $\bar{\Lambda}$  and is normalized to one, so it has a typical size of  $1/\bar{\Lambda} \sim 1/\Lambda$ . There is an additional factor of  $1/\Lambda$  for each derivative of the shape function, from which we expect the naive scaling like  $f(\bar{\Lambda}) \sim 1/\Lambda$ ,

$f'(\bar{\Lambda}) \sim 1/\Lambda^2$ . The constraint from the scaling behavior of the soft form factor does not allow this naive scaling. In fact,  $f(\bar{\Lambda})$  is suppressed by  $\Lambda^2$  and  $f'(\bar{\Lambda})$  is suppressed by  $\Lambda$  compared to the naive scaling behavior due to this constraint. Practically we put  $f(\bar{\Lambda}) = 0$  since it is suppressed by  $\Lambda^2$  compared to the naive scaling behavior, and assume that the series in Eq. (23) converges rapidly such that we choose the terms with the first derivative. However this scaling behavior, especially  $f'(\bar{\Lambda}) \sim 1/\Lambda$  puts a constraint on the endpoint behavior for the shape function models.

We can estimate the size of  $\zeta_P$  from Eq. (21) given a model of the shape function. We adopt the model of Ref. [12], which is given as

$$f(\omega) = \frac{b^b}{\bar{\Lambda}\Gamma(b)} \left(1 - \frac{\omega}{\bar{\Lambda}}\right)^{b-1} e^{b(\omega/\bar{\Lambda}-1)}, \quad (24)$$

at leading order in  $\alpha_s$ . The constraint that the first derivative scales as  $1/\Lambda_{\text{QCD}}$  implies that  $b > 2$  for this model. The default choice of parameters in Ref. [12] is  $\bar{\Lambda} = 0.63$  GeV and  $b = 2.93$ , consistent with this constraint. With this choice of the parameters, and using  $w_s = 4m_\pi^2/m_b = 0.016$  GeV,  $w_M = 0.5$  GeV, we obtain

$$\zeta_P \approx 0.01 \sqrt{\frac{m_B}{\bar{n} \cdot p}}. \quad (25)$$

On the other hand, if we choose  $w_s$  as 0.05 GeV, which can be considered as a typical scale  $\Lambda_{\text{QCD}}^2/m_b$  with  $\Lambda_{\text{QCD}} \sim 0.5$  GeV, we get

$$\zeta_P \approx 0.045 \sqrt{\frac{m_B}{\bar{n} \cdot p}}. \quad (26)$$

The behavior of  $\zeta_P$  with respect to  $w_s$  and  $b$  is illustrated in Fig. 2. The soft form factor  $\zeta_P$  with the input parameter  $b = 2.93$  is smaller than 0.1 in the region  $w_s = [0, 0.1]$  GeV and the central value is  $\zeta_P \sim 0.05$ . However, when we set the input parameter  $b = 2.0$ , the soft

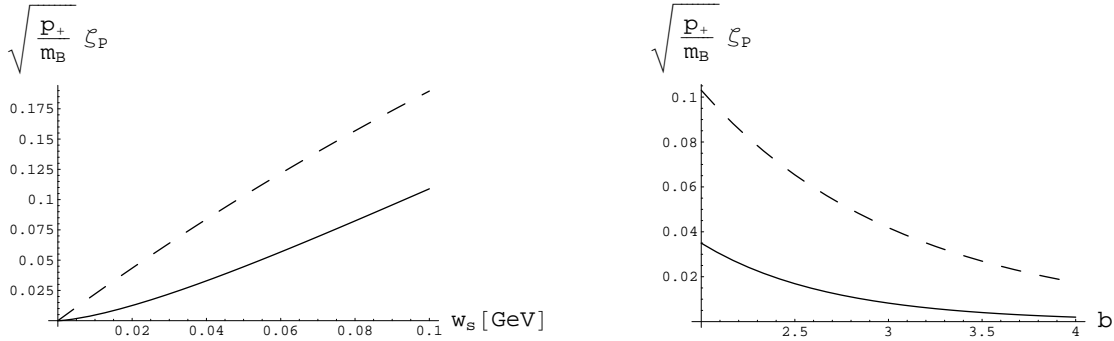


FIG. 2: Dependence of  $\zeta_P$  on the input parameter  $w_s$  and  $b$ . In the first plot, the solid line denotes the soft form factor with  $b = 2.93$  and the dashed line with  $b = 2.00$ . In the second plot, the solid line represents the variation on  $b$  with  $w_s = 0.016$  GeV and the dashed line with  $w_s = 0.05$  GeV.

form factor can be enhanced almost three times compared with the case of  $b = 2.93$ . This can be easily understood when we consider Eqs. (23) and (24). In the case with  $b = 2$ , the shape function in Eq. (24) scales as  $f'(\bar{\Lambda}) \sim 1/\Lambda^2$ , which makes  $\zeta_P \sim \Lambda$  overestimating the scaling behavior. The shape function model in Eq.(24) with  $b \sim 3$  is reliable considering the scaling behavior of  $\zeta_P$  near the tail of the shape function.

We can estimate the size of the soft form factor using the shape function model extracted from  $B \rightarrow X_s \gamma$  [8]. The central fitted values on the exponential model of the shape function in Eq. (24) are

$$\bar{\Lambda} = 0.545 \text{ GeV}, \quad \lambda_1 = -0.342 \text{ GeV}^2, \quad (27)$$

where  $\lambda_1$  is defined as  $\langle \bar{B}_v | \bar{h}_v (n \cdot i D_{us})^2 h_v | \bar{B}_v \rangle = -\lambda_1/3$  and, using the relation [7]

$$\int d\omega \omega^2 f(\omega) = \frac{\bar{\Lambda}^2}{b} = -\frac{\lambda_1}{3}, \quad (28)$$

we can obtain the value of the input parameter  $b = 2.605$  under the choice of Eq. (27). Using the fitted shape function from the data on  $B \rightarrow X_s \gamma$ , the soft form factor at tree level with  $1\sigma$  error is given by

$$\sqrt{\frac{\bar{n} \cdot p}{m_B}} \zeta_P = \begin{cases} 0.0175^{+0.0342}_{-0.0167} & (w_s = 0.016 \text{ GeV}), \\ 0.0710^{+0.0540}_{-0.0580} & (w_s = 0.05 \text{ GeV}). \end{cases} \quad (29)$$

The behavior of  $\zeta_P$  using this shape function model is shown in Fig. 3. In the heavy-to-light soft form factor such as  $\zeta_P$ , it is reasonable to choose  $w_s$  as  $4m_\pi^2/m_b$  since the invariant mass squared of the lowest continuum state starts at  $p^2 \sim 4m_\pi^2$ . Therefore, with this choice of

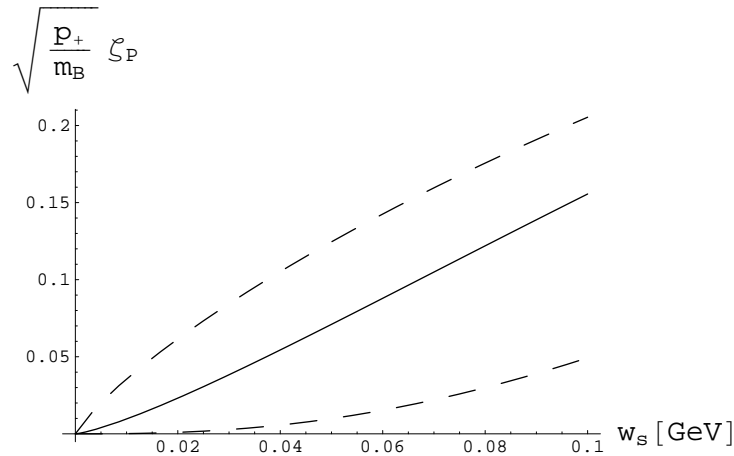


FIG. 3: Tree-level estimate of  $\zeta_P$  with the fitted input parameters extracted from the  $B \rightarrow X_s \gamma$  data. The solid line shows the soft form factor with the central fitted parameters ( $\bar{\Lambda} = 0.545 \text{ GeV}$ ,  $\lambda_1 = -0.342 \text{ GeV}^2$ ). The two dashed lines represent the range of the soft form factor with  $1\sigma$  error, where the upper line is obtained with the input parameters ( $\bar{\Lambda} = 0.781 \text{ GeV}$ ,  $\lambda_1 = -1.13 \text{ GeV}^2$ ), and the lower line with  $\bar{\Lambda} = 0.485 \text{ GeV}$ ,  $\lambda_1 = -0.13 \text{ GeV}^2$ .

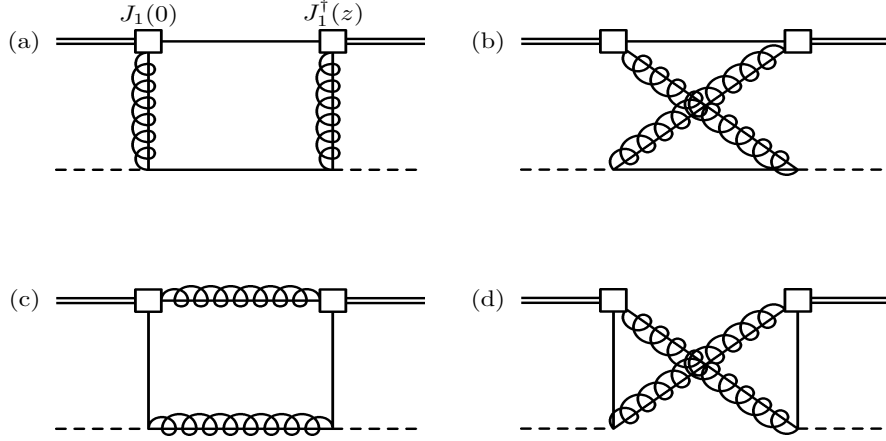


FIG. 4: Feynman diagrams for the lowest-order contributions to  $\Pi_1(q)$  in SCET<sub>I</sub>.

$w_s$ , we find  $\zeta_P(B \rightarrow \pi)$  at tree level can be small contrary to the prediction of the QCD factorization approach [13, 14].

The numerical analysis of the soft form factor  $\zeta_P$  is based on the tree-level relation in Eq. (21). There can be a few sources of theoretical uncertainties. For example, there may be uncertainties in choosing the Borel parameters  $w_s$  and  $w_M$ . Since the forward scattering is computed in SCET<sub>I</sub>, the virtuality of the intermediate state, or the pion state is of order  $M^2 = w_M \bar{n} \cdot p \sim m_b \Lambda$ , and  $w_M \sim \Lambda$ . And  $w_s$  is the scale from which the continuum states start. We take as  $w_s = 4m_\pi^2/\bar{n} \cdot p$  or  $\sim \Lambda^2/m_b$  with  $\Lambda \approx 0.5$  GeV, assuming that  $m_\pi^2 \sim \Lambda^2$ , which is obviously an overestimation. This is in contrast to the choice of the Borel parameters in Ref. [4], in which they take  $w_s \approx w_M \approx 0.2$  GeV. Their tree-level evaluation of the soft form factor corresponds to  $\zeta_P \sim 0.32$ , while our evaluation is about 0.01 ( $w_s = 0.016$  GeV) and 0.05 ( $w_s = 0.05$  GeV), which is smaller by an order of magnitude. We find that the variation of  $w_M$  between 0.2 GeV and 0.6 GeV gives 1% ( $w_s = 0.016$  GeV), 10% ( $w_s = 0.05$  GeV). Therefore we can argue that the large uncertainty arises from the choice of  $w_s$ . Indeed, we obtain  $\zeta_P \approx 0.30$  in our evaluation with  $w_s = 0.2$  GeV,  $w_M = 0.4$  GeV, close to the result in Ref. [4].

Let us briefly comment on the higher-order corrections to the tree-level relation in Eq. (21). First, we have to include the radiative correction to  $\Pi(q)$ , which include the radiative corrections of  $J_0$ . In addition, we also have to include the spectator interactions. When we consider a hard collinear gluon exchange with the spectator quark, the contributions can be separated into two parts, the soft form factor  $\zeta_P$  and the hard form factor  $\zeta_J$ , based on the existence of the spin symmetry of the heavy-to-light current [11, 14]. The hard spectator contributions for  $\zeta_P$  satisfying the spin symmetry can be distinguished simply by the presence of the leading order current  $J_0$  in the time-ordered product [9]. In this case we need to include the higher order interaction terms of SCET<sub>I</sub> collinear Lagrangian in the correlation function.



The spin symmetry breaks down explicitly if subleading currents with  $i\mathcal{D}_c^\perp$  are included in the time-ordered product. Therefore, when the hard spectator contributions for  $\zeta_J$  are considered, we have to define a correlation function with the subleading current  $J_1$ , which is given by

$$J_1(x) = e^{i(\bar{p}-m_b v)\cdot x} \bar{\xi}_n \frac{\not{n}}{2} i\mathcal{D}_c^\perp W Y^\dagger h_v(x). \quad (30)$$

In this case, the intermediate state consists of hard-collinear particles and one of the correlation functions is given by

$$\Pi_1(q^2) = i \int d^4 z e^{iq\cdot z} \int d^4 x \int d^4 y \langle \bar{B} | T [J_1^\dagger(z) J_1(0) i\mathcal{L}_{\xi q}^{(1)}(x) i\mathcal{L}_{\xi q}^{(1)}(y)] | \bar{B} \rangle, \quad (31)$$

where  $\mathcal{L}_{\xi q}^{(1)} = \bar{\xi}_n (\not{P}^\perp + gA_n^\perp) W Y^\dagger q_{us}$  is the ultrasoft-collinear Lagrangian. This correlation function contributes to the hard form factor. After integrating out the hard-collinear degrees of freedom, we have four-quark operators with  $h_v$  and  $q_{us}$ . As seen in Fig. 4, from the four possible contractions of the hard-collinear particles in the intermediate state we obtain the operators in SCET<sub>II</sub> of the form

$$\begin{aligned} O_1(l_1^+, l_2^+) &= (\bar{h}Y)_a \frac{\not{n}}{2} \delta(l_1^+ - n \cdot i\partial) (Y^\dagger h)_b \cdot (\bar{q}_{us}Y)_b \frac{\not{n}}{2} \delta(l_2^+ - n \cdot i\partial) (Y^\dagger q_{us})_a, \\ O_2(l_1^+, l_2^+) &= (\bar{h}Y)_a \frac{\not{n}}{2} \sigma_{\perp\alpha\beta} \delta(l_1^+ - n \cdot i\partial) (Y^\dagger h)_b \cdot (\bar{q}_{us}Y)_b \frac{\not{n}}{2} \sigma_{\perp}^{\alpha\beta} \delta(l_2^+ - n \cdot i\partial) (Y^\dagger q_{us})_a, \\ O_3(l_1^+, l_2^+) &= (\bar{h}Y)_a \frac{\not{n}\not{n}}{4} \delta(l_1^+ - n \cdot i\partial) (Y q_{us})_a \cdot (\bar{q}_{us}Y)_b \frac{\not{n}\not{n}}{4} \delta(l_2^+ - n \cdot i\partial) (Y^\dagger h)_b, \\ O_4(l_1^+, l_2^+) &= (\bar{h}Y)_a \frac{\not{n}\not{n}}{4} \sigma_{\perp\alpha\beta} \delta(l_1^+ - n \cdot i\partial) (Y q_{us})_a \cdot (\bar{q}_{us}Y)_b \frac{\not{n}\not{n}}{4} \sigma_{\perp}^{\alpha\beta} \delta(l_2^+ - n \cdot i\partial) (Y^\dagger h)_b, \end{aligned} \quad (32)$$

where  $\sigma_{\perp}^{\alpha\beta} = i[\gamma_{\perp}^\alpha, \gamma_{\perp}^\beta]/2$ , and  $a, b$  are color indices. In addition, we also have to consider the possibilities that the hard-collinear loop diagrams in Fig. 4 can be matched onto the nonlocal time-ordered products such as Fig. 5 in SCET<sub>II</sub>. When calculating the hard-collinear loop corrections, we are confronted with non-vanishing infrared divergences which result from internal propagators with virtualities of order  $\Lambda^2$ . In this case we expect the infrared divergences will be reproduced by the possible nonlocal time-ordered products in SCET<sub>II</sub>.

Therefore, by matching onto SCET<sub>II</sub>, we obtain

$$\begin{aligned} \Pi_1 &= \int dl_1^+ dl_2^+ \sum_{i=1}^4 J_i(\bar{n} \cdot p, n \cdot r, l_1^+, l_2^+) \langle \bar{B} | O_i(l_1^+, l_2^+) | \bar{B} \rangle \\ &\quad + \int d^4 x d^4 y \sum_{i,k} J'_i J'_k \otimes \langle \bar{B} | T [O_i^L(x), O_k^L(y)] | \bar{B} \rangle + \dots, \end{aligned} \quad (33)$$

where  $J_i, J'_i$  are the jet functions and  $\otimes$  denotes convolutions of  $l_i^+, l_k^+$  which can appear in the operators  $O_i^L, O_k^L$ . The matrix elements between the  $B$  meson in Eq. (33) are new non-perturbative parameters to be included by defining additional subleading shape functions of the  $B$  meson. Similarly, there are also hard spectator contributions to  $\zeta_P$  from other

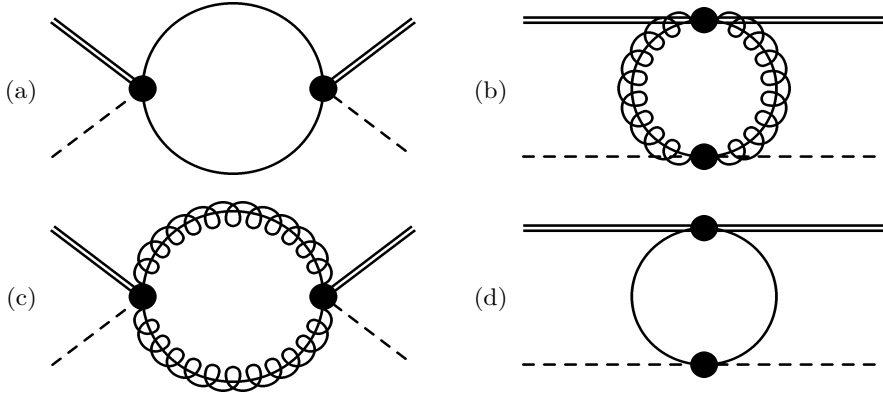


FIG. 5: Examples on the nonlocal time-ordered products in  $\text{SCET}_{\text{II}}$ . The internal loops consist of the collinear particles with offshellness  $\Lambda^2$ . The dotted vertices denote the four-particle operators obtained from the matching respectively by integrating out the hard-collinear gluons (a,d) and quark fields (b,c).

time-ordered products with the subleading collinear Lagrangian, which introduce more non-perturbative parameters. However, we have no information on these subleading  $B$  meson shape functions, and hence we do not further consider higher-order corrections and other theoretical uncertainties such as the renormalization scale dependence in this paper.

We have derived the tree-level relation between the soft form factor for  $B \rightarrow \pi$  and the leading  $B$  meson shape function using the sum rule approach. This is achieved by considering the forward scattering amplitude of the heavy-to-light current near the endpoint. We derived a constraint on the behavior of the  $B$  meson shape function near the endpoint using the scaling behavior of the soft form factor,  $\zeta_P \sim (\Lambda/m_b)^{3/2}$ . Since we work at tree level only, there may be a lot of uncertainties, and there may also be a model dependence on the form of the shape function. But the analysis suggests that the soft form factor can be about 0.01 to 0.07, considering various inputs from the models and using the experimental data on the  $B$  meson shape function. The numerical value of the soft form factor is approximately smaller by an order of magnitude than other sum rule predictions. Since we have not included higher-order corrections in  $\alpha_s$ , this evaluation may have a large theoretical uncertainty, but our analysis favors a small value of the soft form factor.

## Acknowledgments

We thank Ed Thorndike for his help in providing the parameters for the experimentally extracted shape function. We also thank the Institute for Nuclear Theory at the University of Washington for its hospitality and the Department of Energy for partial support during

the completion of this work. J. Chay was supported by Grant No. R01-2002-000-00291-0 from the Basic Research Program of the Korea Science & Engineering Foundation. C. Kim and A. K. Leibovich were supported by the National Science Foundation under Grant No. PHY-0244599. A. K. Leibovich was also supported in part by the Ralph E. Powe Junior Faculty Enhancement Award.

- 
- [1] C. W. Bauer, I. Z. Rothstein and I. W. Stewart, Phys. Rev. Lett. **94** (2005) 231802; M. Beneke, G. Buchalla, M. Neubert and C. T. Sachrajda, arXiv:hep-ph/0411171; C. W. Bauer, D. Pirjol, I. Z. Rothstein and I. W. Stewart, arXiv:hep-ph/0502094.
  - [2] M. Okamoto *et al.*, Nucl. Phys. Proc. Suppl. **140** (2005) 461; J. Shigemitsu *et al.*, arXiv:hep-lat/0408019.
  - [3] P. Ball and R. Zwicky, JHEP **0110** (2001) 019; Phys. Rev. D **71** (2005) 014015.
  - [4] F. De Fazio, T. Feldmann and T. Hurth, arXiv:hep-ph/0504088.
  - [5] P. Ball, arXiv:hep-ph/0308249.
  - [6] C. W. Bauer, S. Fleming and M. E. Luke, Phys. Rev. D **63** (2001) 014006; C. W. Bauer, S. Fleming, D. Pirjol and I. W. Stewart, Phys. Rev. D **63** (2001) 114020; C. W. Bauer, D. Pirjol and I. W. Stewart, Phys. Rev. D **65** (2002) 054022.
  - [7] M. Neubert, Phys. Rev. D **49** (1994) 3392; T. Mannel and M. Neubert, Phys. Rev. D **50** (1994) 2037.
  - [8] A. Bornheim *et al.* [CLEO Collaboration], Phys. Rev. Lett. **88** (2002) 231803.
  - [9] C. W. Bauer, D. Pirjol and I. W. Stewart, Phys. Rev. D **67** (2003) 071502.
  - [10] V. L. Chernyak and I. R. Zhitnitsky, Nucl. Phys. B **345** (1990) 137.
  - [11] M. Beneke, G. Buchalla, M. Neubert and C. T. Sachrajda, Nucl. Phys. B **591** (2000) 313.
  - [12] S. W. Bosch, B. O. Lange, M. Neubert and G. Paz, Nucl. Phys. B **699** (2004) 335; S. W. Bosch, M. Neubert and G. Paz, JHEP **0411** (2004) 073.
  - [13] M. Beneke, G. Buchalla, M. Neubert and C. T. Sachrajda, Phys. Rev. Lett. **83** (1999) 1914.
  - [14] M. Beneke and T. Feldmann, Nucl. Phys. B **592** (2001) 3.